NASA/TM-2002-210719

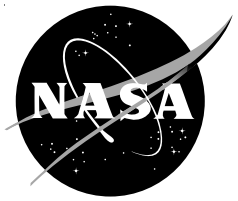

# In-Flight Vibration Environment of the NASA F-15B Flight Test Fixture

*Stephen Corda, Russell J. Franz, James N. Blanton, M. Jake Vachon, and James B. DeBoer*
*NASA Dryden Flight Research Center*
*Edwards, California*

**February 2002**

## The NASA STI Program Office…in Profile

Since its founding, NASA has been dedicated to the advancement of aeronautics and space science. The NASA Scientific and Technical Information (STI) Program Office plays a key part in helping NASA maintain this important role.

The NASA STI Program Office is operated by Langley Research Center, the lead center for NASA's scientific and technical information. The NASA STI Program Office provides access to the NASA STI Database, the largest collection of aeronautical and space science STI in the world. The Program Office is also NASA's institutional mechanism for disseminating the results of its research and development activities. These results are published by NASA in the NASA STI Report Series, which includes the following report types:

- TECHNICAL PUBLICATION. Reports of completed research or a major significant phase of research that present the results of NASA programs and include extensive data or theoretical analysis. Includes compilations of significant scientific and technical data and information deemed to be of continuing reference value. NASA's counterpart of peer-reviewed formal professional papers but has less stringent limitations on manuscript length and extent of graphic presentations.

- TECHNICAL MEMORANDUM. Scientific and technical findings that are preliminary or of specialized interest, e.g., quick release reports, working papers, and bibliographies that contain minimal annotation. Does not contain extensive analysis.

- CONTRACTOR REPORT. Scientific and technical findings by NASA-sponsored contractors and grantees.

- CONFERENCE PUBLICATION. Collected papers from scientific and technical conferences, symposia, seminars, or other meetings sponsored or cosponsored by NASA.

- SPECIAL PUBLICATION. Scientific, technical, or historical information from NASA programs, projects, and mission, often concerned with subjects having substantial public interest.

- TECHNICAL TRANSLATION. English-language translations of foreign scientific and technical material pertinent to NASA's mission.

Specialized services that complement the STI Program Office's diverse offerings include creating custom thesauri, building customized databases, organizing and publishing research results…even providing videos.

For more information about the NASA STI Program Office, see the following:

- Access the NASA STI Program Home Page at ***http://www.sti.nasa.gov***

- E-mail your question via the Internet to help@sti.nasa.gov

- Fax your question to the NASA Access Help Desk at (301) 621-0134

- Telephone the NASA Access Help Desk at (301) 621-0390

- Write to:
  NASA Access Help Desk
  NASA Center for AeroSpace Information
  7121 Standard Drive
  Hanover, MD 21076-1320

NASA/TM-2002-210719

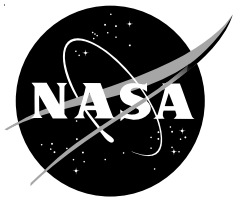

# In-Flight Vibration Environment of the NASA F-15B Flight Test Fixture

*Stephen Corda, Russell J. Franz, James N. Blanton, M. Jake Vachon, and James B. DeBoer*
*NASA Dryden Flight Research Center*
*Edwards, California*

National Aeronautics and
Space Administration

Dryden Flight Research Center
Edwards, California 93523-0273

**February 2002**

## NOTICE

Use of trade names or names of manufacturers in this document does not constitute an official endorsement of such products or manufacturers, either expressed or implied, by the National Aeronautics and Space Administration.

Available from the following:

NASA Center for AeroSpace Information (CASI)
7121 Standard Drive
Hanover, MD 21076-1320
(301) 621-0390

National Technical Information Service (NTIS)
5285 Port Royal Road
Springfield, VA 22161-2171
(703) 487-4650

## ABSTRACT

Flight vibration data are analyzed for the NASA F-15B/Flight Test Fixture II test bed. Understanding the in-flight vibration environment benefits design and integration of experiments on the test bed. The power spectral density (PSD) of accelerometer flight data is analyzed to quantify the in-flight vibration environment from a frequency of 15 Hz to 1325 Hz. These accelerometer data are analyzed for typical flight conditions and maneuvers. The vibration data are compared to flight-qualification random vibration test standards. The PSD levels in the lateral axis generally are greater than in the longitudinal and vertical axes and decrease with increasing frequency. At frequencies less than approximately 40 Hz, the highest PSD levels occur during takeoff and landing. Peaks in the PSD data for the test fixture occur at approximately 65, 85, 105–110, 200, 500, and 1000 Hz. The pitch-pulse and 2-*g* turn maneuvers produce PSD peaks at 115 Hz. For cruise conditions, the PSD level of the 85-Hz peak is greatest for transonic flight at Mach 0.9. From 400 Hz to 1325 Hz, the takeoff phase has the highest random vibration levels. The flight-measured vibration levels generally are substantially lower than the random vibration test curve.


## NOMENCLATURE

| | |
|---|---|
| $D$ | dimension, ft |
| $f_s$ | frequency of vortex shedding, Hz |
| FTF–II | Flight Test Fixture II |
| $g$ | gravitational acceleration constant, 32.174 ft/sec$^2$ |
| *KIAS* | indicated airspeed, knots |
| PSD | power spectral density, $g^2$/Hz |
| RMS | root mean square |
| $S$ | Strouhal number, $S = f_s D / V$ |
| $V$ | free-stream velocity, ft/sec |

## INTRODUCTION

The NASA Dryden Flight Research Center (Edwards, California) F-15B/Flight Test Fixture II (FTF–II) test bed (fig. 1 and ref. 1) is used to flight-test a variety of flight research experiments. Flight research is conducted in several areas, including aerodynamics, structural dynamics, instrumentation, sensor development, advanced video techniques, and propulsion. All experiment hardware must be flight-qualified prior to flight to verify functional operability and to ensure no failure modes detrimental to flight safety exist.

One flight qualification requirement for experiment hardware is the successful completion of a random vibration test. The current NASA requirement is a shake test with the acceleration power spectral density (PSD) as a function of frequency schedule, as shown in figure 2 from reference 2. For flight on the F-15B/FTF–II test bed, hardware typically is shaken to either “curve A” or “curve B” (fig. 2). The

vibration is applied to each of the three mutually perpendicular axes of the hardware in separate tests. The hardware is tested with random vibration for a minimum of 20 min in each axis.

An attempt has been made to quantify the actual F-15B/FTF–II in-flight random vibration environment. Flight data have been analyzed for a variety of flight conditions and maneuvers including taxi; takeoff; climb; straight-and-level flight at subsonic, transonic, and supersonic speeds; level 2-*g* turns; pitch pulses; sideslips; descent; and landing.

## AIRPLANE AND FLIGHT TEST FIXTURE II DESCRIPTION

The F-15B aircraft is a two-seat fighter/trainer version of the F-15 high-performance, supersonic, air-superiority fighter aircraft (McDonnell Aircraft Company, now The Boeing Company, St. Louis, Missouri). The aircraft is powered by two F100-PW-100 turbofan engines with afterburners manufactured by Pratt & Whitney (West Palm Beach, Florida). Each engine has an uninstalled, sea-level, static thrust rating of approximately 25,000 lbf. The F-15B aircraft is 63.7-ft long and has a wingspan of 42.8 ft (fig. 3). The aircraft has a basic operating weight of 27,500 lb and a takeoff gross weight of 54,000 lb.

The NASA F-15B airplane has been converted from its U. S. Air Force role as an air-superiority fighter to a research test bed aircraft. This conversion includes the installation of research instrumentation, recording, telemetry, and video systems. A significant feature of the research capability of the aircraft is its ability to carry the FTF–II. The FTF–II is installed on the F-15B centerline pylon similar to the installation of an operational centerline fuel tank (figs. 3–4). The FTF–II is a second-generation research fixture; the first flight test fixture was flown on a NASA F-104 aircraft (ref. 3).

The FTF–II is a low-aspect-ratio, fin-like shape with an elliptical nose section and blunt base. The fixture is 107.0-in. long, 32.0-in. high, and 8.0-in. wide (fig. 4). The FTF–II is constructed of composites and has a modular configuration. The fixture has a research instrumentation section; and the replaceable nose section, side panels, and vertical section provide the flexibility to integrate a variety of flight test experiments and configurations. The maximum allowable weight of the FTF–II, including research systems, is 500 lb. Steady-state performance limits of the F-15B/FTF–II configuration include a maximum altitude of 60,000 ft; airspeeds to a maximum of 600 knots indicated airspeed (*KIAS*) (equivalent to a dynamic pressure of approximately 1000 lbf/ft$^2$); and a Mach number of 2.0. Reference 1 provides further details about the FTF–II.

## INSTRUMENTATION AND DATA ANALYSIS

Ten-bit acceleration data have been obtained from two Endevco Corporation (San Juan Capistrano, California) ISOTRON® model 5253A-100 triaxial accelerometers located in the FTF–II. The accelerometers are mounted on the vertical and lateral centerlines of the FTF–II at two different longitudinal stations. The accelerometers are located 58.9 in. and 93.1 in. aft of the FTF–II leading edge (55 and 87 percent of the FTF–II geometric chord length, respectively).

A digital data acquisition and telemetry system recorded accelerations in the longitudinal, lateral, and vertical axes. The sample rates for the accelerometers located at the 55- and 87-percent chord locations

were 10,416 samples/sec and 801 samples/sec, respectively. Hence, the 801-Hz and 10,416-Hz accelerometer data are referred to as the low-speed data and the high-speed data, respectively. The low-speed data were filtered with a three-pole Butterworth antialiasing filter that has a 3-dB down point at 160 Hz. The high-speed data were filtered with a three-pole Butterworth antialiasing filter that has a 3-dB down point at 1325 Hz. Because of the filtering, the low-speed and high-speed data have been analyzed to maximum frequencies of 160 Hz and 1325 Hz, respectively. Table 1 contains specifications for the accelerometer.

Table 1. Accelerometer specifications.

| Characteristics | Specifications |
|---|---|
| Full-scale range | ± 25 *g* |
| Resolution | 0.049 *g* |
| Accuracy | ± 10 percent* |
| Sample rate | 801 Hz (low speed) |
| | 10,416 Hz (high speed) |
| Frequency response | 2–10,000 Hz |
| Three-pole Butterworth antialiasing filter cutoff frequency | 160 Hz (low speed) |
| | 1325 Hz (high speed) |

* Main limitations are cross-axis sensitivity and frequency dependence.

Time slices of flight data have been analyzed for each representative condition or maneuver. The time slices are 1 min in length for steady flight conditions and varied for maneuvers. The MATLAB® software (The MathWorks, Inc., Natick, Massachusetts) (ref. 4) has been used to calculate the PSD for the specified sampling frequency at 1-Hz resolution. The spectral density has been plotted as a function of frequency to describe the random vibration environment for the F-15B/FTF–II configuration during various flight conditions and maneuvers.

## Time-Domain Data

Figure 5 shows typical time-domain data for a complete flight profile. Mach number; altitude; angles of attack and sideslip; and longitudinal, lateral, and vertical acceleration are plotted as a function of time for flight number 165. Flight conditions and maneuvers are labeled. The accelerometers measured the excitation from the equilibrium condition: 0 *g* for the axial and lateral axes and –1 *g* for the vertical axis. Note that the maximum accelerations were approximately 0.5 *g* for the longitudinal axis, 2.0 *g* for the lateral axis, and 1.0 *g* for the vertical axis. The excitation was largest in the lateral axis, then in the vertical axis. Little excitation was seen in the longitudinal axis.

An accelerometer was affixed to an electrodynamic shaker programmed to generate curve A accelerations. Figure 6 shows the average of PSDs over 30 sec for the 10,416-Hz data. Deviations from the programmed curve were caused by the precision of the shaker control and the resolution and accuracy of the accelerometer.

Figure 7 shows the longitudinal, lateral, and vertical acceleration PSD levels as a function of frequency for a typical takeoff and landing. For reference, the PSD for NASA Dryden flight qualification shake test curves are shown. The acceleration in the lateral axis was dominant over most of the frequency range for takeoff and landing. Based on a review of the data in all three axes, the lateral axis acceleration was found to be dominant for most of the flight conditions and maneuvers analyzed except for taxi, the pitch pulses, and the 2-*g* turns, in which the vertical axis accelerations were also significant.

## FLIGHT TEST RESULTS AND DISCUSSION

Flight test data have been analyzed from five separate F-15B/FTF–II flights: flight numbers 143, 144, 154, 155, and 165. Low-speed accelerometer data have been analyzed for all of these flights. The high-speed data were obtained for portions of flight 144 only. These flights are representative of the random vibration environment typically encountered by the F-15B/FTF–II test bed. Tables 2 and 3 show all of the flight conditions and maneuvers analyzed from these flights.

Steady-state flight conditions analyzed were taxi; takeoff; climb; straight-and-level flight at subsonic, transonic, and supersonic speeds; descent; and landing. The flight maneuvers analyzed include pitch pulses, 2-*g* turns, and sideslips with the landing gear up and down. Not all of these conditions and maneuvers were present in each flight. The subsonic cruising conditions were Mach 0.5, 0.6, 0.7, 0.8, and 0.9 in level flight at an altitude of 15,000 ft. The supersonic cruising conditions were Mach 1.0, 1.3, and 1.4 in level flight at an altitude of 30,000 ft. The flight maneuver data were collected at altitudes of 10,000 ft, 15,000 ft, and 20,000 ft.

### Steady-State Flight Conditions Data

Figures 8–18 show PSD data as a function of frequency for the steady-state flight conditions. The PSD data are shown for taxi; takeoff; climb; level subsonic, transonic, and supersonic flight; descent; and landing. All of the figures show the NASA Dryden flight qualification test curves for random vibration. For all of the flight data, the maximum value of spectral density generally is an order of magnitude or more below the curve B value at low frequency and several orders of magnitude lower at high frequency. The data show a low-frequency structural mode of approximately 10–15 Hz. For many of the cases, peaks exist in the PSD data at approximately 65, 85, 100–105, 200, and 500 Hz; perhaps indicating resonant frequencies of the FTF–II itself.

Figure 8 shows the lateral and vertical acceleration PSD data for taxi. Two curves are shown for each axis: a preflight curve and a postflight curve. The preflight curve corresponds to the aircraft taxiing before takeoff at a fully fueled weight of approximately 40,000 lb. The postflight curve corresponds to a postflight taxi weight of approximately 30,000 lb. The preflight and postflight results are comparable in magnitude for each axis, but the PSD of the vertical axis is approximately 5 times greater than that of the lateral axis for frequencies greater than 20 Hz. The vertical and lateral axis PSD levels are on the order of $10^{-5}$ $g^2$/Hz and $10^{-6}$ $g^2$/Hz, respectively. Distinct peaks in the PSD for both cases are at approximately 55, 65, and 105 Hz.

Table 2. Analyzed flight conditions.

| Steady-state flight condition | Flight number | Mach number | Altitude, kft |
|---|---|---|---|
| Taxi | 165 | - | - |
| Takeoff | 143 | - | - |
| | 144* | | |
| | 165 | - | - |
| Climb | 143 | 0.4 | 10–16 |
| | 144* | 0.4 | 10–15 |
| | 165 | 0.7 | 10–18 |
| Level subsonic flight | 143 | 0.4 | 20 |
| | 143 | 0.5 | 20 |
| | 144* | 0.5 | 20 |
| | 154 | 0.5 | 15 |
| | 144* | 0.6 | 20 |
| | 154 | 0.6 | 15 |
| | 144* | 0.7 | 20 |
| | 154 | 0.7 | 15 |
| Level transonic flight | 154 | 0.8 | 15 |
| | 154 | 0.9 | 15 |
| | 155 | 1.0 | 34 |
| Level supersonic flight | 154 | 1.3 | 30 |
| | 165 | 1.4 | 34 |
| Descent | 143 | 0.4 | 13–10 |
| | 144* | 0.4 | 14–11 |
| | 165 | 0.6 | 21–16 |
| Landing | 143 | - | - |
| | 144* | - | - |
| | 165 | - | - |

*High- and low-speed data analyzed

Table 3. Analyzed flight maneuvers.

| Flight maneuvers | Flight number | Mach number | Altitude, kft |
|---|---|---|---|
| Sideslip, landing gear down | 165 | 0.4 | 15 |
| Sideslip, landing gear up | 165 | 0.4 | 15 |
| Pitch pulse | 143 | 0.4 | 20 |
| 2-$g$ turn | 143 | 0.4 | 10 |

Figure 9 shows the lateral acceleration PSD calculated from the low- and high-speed data for takeoff. As previously mentioned, the low- and high-speed data are calculated and plotted to frequencies of 160 Hz and 1325 Hz, respectively. The takeoff data includes the high-speed takeoff roll on the runway, followed by nosewheel rotation, main landing gear liftoff, and initial climb. The takeoff excites the low-frequency structural mode at approximately 10–15 Hz, reaching levels of approximately 0.03 $g^2$/Hz. Peaks in the low-speed PSD data are at frequencies of approximately 65, 85, and 105 Hz. The high-speed data show PSD peaks at approximately 65, 85, 105, 130, 200, and 500 Hz. The high-frequency peaks correspond to the vibration range associated with the aircraft jet engines.

The low-frequency PSD, between approximately 10 and 50 Hz, is significantly higher for the takeoff and landing data than for other steady-state data. This excitation may be caused by vortex shedding from the nosewheel landing gear door that is extended during takeoff and landing. For takeoff and landing, the Reynolds number, based on the nosewheel door width of approximately 15 in., is on the order of $10^5$ to $10^6$. The Strouhal number, $S$, for a flat plate over this Reynolds number range varies from approximately 0.13 to 0.20 (ref. 5). Based on the definition of $S$, the frequency of vortex shedding, $f_s$, can be calculated as $f_s = SV/D$ ; where $V$ is the free-stream velocity and $D$ is the characteristic dimension, here the nosewheel landing gear door width (in ft). Based on the above assumptions, the $f_s$ from the nosewheel landing gear door for takeoff and landing is estimated to be between approximately 10 and 40 Hz.

Figure 10 shows the lateral acceleration PSD data for steady climbing flight. The data are for a nominal 350-kn climb. Resonant frequencies at approximately 65, 85, and 105 Hz in the low- and high-speed data are more evident for the climb data than for the takeoff data. The high-speed data also show PSD peaks at approximately 200 Hz, again in the jet engine frequency range. Comparing the climb data with the takeoff data, the takeoff PSD data show more energy in the low-frequency range to approximately 50 Hz, again perhaps because of the effects of the nosewheel landing gear door.

Spectral density at constant Mach numbers from Mach 0.5 to Mach 1.4 and steady altitude has been analyzed. Figure 11 shows lateral acceleration PSD data for subsonic flight at Mach 0.5, 0.6, 0.7, 0.8, and 0.9. The vibration level increases with Mach number level, increasing by an order of magnitude from Mach 0.5 to Mach 0.9. This trend is probably caused by the increase in flow turbulence under the aircraft as the airspeed increases. Noticeable peaks in the PSD are seen in all of the subsonic flight data at frequencies of approximately 80 and 105–110 Hz. The PSD reaches a maximum at approximately Mach 0.9, but still well below the limit of test curve B. Figure 12 shows the lateral acceleration PSD data for level flight at Mach 0.5 from the low- and high-speed data. The PSD peaks are seen at approximately 65, 85, 110, 200, and 500 Hz.

Figure 13 shows lateral acceleration PSD data for level transonic flight. The general increase in PSD from Mach 0.8 to Mach 0.9 is followed by a dramatic decrease in PSD from Mach 0.9 to Mach 1.0. The PSDs at Mach 0.9 and Mach 1.0 show more distinct peaks at several frequencies than the subsonic flight data do. The PSD decreases further from Mach 1.0 to Mach 1.3. The larger values of PSD at Mach 0.9 are characteristic of transonic dynamic structural responses caused by transonic aerodynamic and structural coupling. Very distinct PSD peaks are seen at 80 Hz and 100–105 Hz.

Figure 14 shows lateral acceleration PSD data for level supersonic flight at Mach 1.3 and Mach 1.4. The PSD values are generally lower than those for the subsonic and transonic flight data, with less defined peaks across the frequency spectrum. The PSD for supersonic flight is approximately two to three orders of magnitude lower than test curve B.

Figure 15(a) shows a three-dimensional plot of the PSDs shown in figures 13 and 14, resulting in a clear view of the growth and decay of a minimum of five resonant frequencies from Mach 0.5 to Mach 1.4. Figure 15(b) shows a planar view from above figure 15(a).

The lateral acceleration PSD plot for descent (fig. 16) is similar to the climbing flight data (fig. 10). Because the descent and climb speeds were approximately the same, this result was expected. Although the magnitudes of the frequency responses are relatively low, resonance peaks are still seen at approximately 65, 85, 100–105, 200, 450, and 950 Hz. The low-frequency PSD levels for flight 165 are much lower than for the other data shown, with significant peaks at approximately 25, 35, and 50 Hz.

Figures 17(a) and 17(b) show the lateral and vertical acceleration PSD plots for landing. The overall random vibration PSD levels for landing generally are larger than for the other flight regimes, except taxi and discrete peaks in the pitch-pulse and 2-*g* turn maneuvers. The PSD plot is again "fuller" from approximately 25 to 40 Hz, perhaps because of vortex shedding from the nosewheel landing gear door. The PSD peaks are at frequencies of approximately 40, 65, 85, 105 and 200–250 Hz. The vertical acceleration PSD has peaks at the higher frequencies of approximately 140, 270, 550, and 1000 Hz. The vertical acceleration PSD, although higher for landing than for the other steady-state flight conditions, is two to three orders of magnitude lower than test curve B.

Figures 18(a) and 18(b) show the lateral acceleration PSD curves for all of the steady-state flight conditions from the low- and high-speed data, respectively. From frequencies of 10 to approximately 40 Hz, the largest PSD levels are from takeoff and landing. Between approximately 40 and 160 Hz, the landing and transonic vibration levels are comparable, with the landing levels decreasing and the transonic flight levels increasing. The transonic flight levels are greatest to approximately 300 Hz. From approximately 300 to 1320 Hz, the takeoff phase produced the largest vibration levels. Qualitatively, for low frequencies, the order of the flight phases for increasing vibration (from lowest to highest) is postflight taxi, preflight taxi, level subsonic flight, descent, climb, level supersonic flight, level transonic flight, takeoff, and landing. All of the vibration levels are well below the test curve values, except at the lowest frequency.

## Flight Maneuvers Data

Flight maneuvers analyzed include 5° steady-heading sideslips, pitch pulses, and level 2-*g* turns. Figures 19–22 show the PSD data as a function of frequency for these flight maneuvers. The maneuvers were performed at approximately Mach 0.4. The altitude for each maneuver varied: 20,000 ft for the pitch-pulse maneuvers, 15,000 ft for the sideslip maneuvers, and 10,000 ft for the 2-*g* turns. Angle-of-sideslip data were obtained with the landing gear up and down.

Figure 19 shows the lateral acceleration PSD for steady-heading sideslips of approximately 5° with both gear up and gear down. As expected, based on the takeoff and landing data, the random vibration levels are much greater with the gear down. The differences in the two curves provide additional quantitative vibration data about the effect of having the landing gear extended. At the airspeed the sideslips were performed, the $f_s$ from the nosewheel landing gear door is estimated to be approximately 40 to 70 Hz. The data obtained with the gear down show a definite energy increase in the 35–70 Hz region. Peaks at approximately 80 and 105 Hz are evident as in the steady-state flight condition data. All of the levels are still well below test curve B levels, except at the lowest frequency.

The pitch-pulse and 2-*g* turn maneuvers produced the largest, discrete PSD peaks encountered in the present study. Figure 20 shows the acceleration pitch pulse data. Significant PSD peaks are seen in the lateral data at approximately 15–20, 50, and 85 Hz; a large spike reaches the test curve levels at approximately 115 Hz.

The lateral and vertical acceleration, 2-*g* turn data are similar to the pitch-pulse data (fig. 21). The 2-*g* load in the vertical axis appears to produce the large peak at approximately 50 Hz in the vertical acceleration data. The large spike at approximately 115 Hz in the lateral acceleration data is similar to the spike seen in the pitch-pulse data. At the low frequencies, the vertical PSD is higher than the lateral components for the 2-*g* turn.

Figure 22 shows the PSD curves of the lateral accelerations for all of the flight maneuvers and the full profile of test curves A–D. The PSD is dominated at the low frequencies by the sideslip maneuver performed with gear down, and the pitch-pulse and 2-*g* turn maneuvers contribute spikes of large magnitudes at the high frequencies. All of the PSD levels for the flight maneuvers are below test curve B levels, although these curves show the potential for large spikes at specific frequencies caused by specific maneuvers.

## CONCLUSIONS

The random vibration environment for the NASA F-15B/Flight Test Fixture II (FTF–II) test bed was studied and quantified using spectral analysis of the fixture-mounted accelerometer data. Power spectral density (PSD) was calculated for acceleration to a maximum frequency of 1325 Hz. All of the calculated random vibration levels for steady-state flight conditions and various flight maneuvers were within the limits defined by the NASA Dryden Flight Research Center flight qualification vibration test "curve B," except for the discrete peak observed at 115 Hz in the pitch-pulse and 2-g maneuvers.

The lateral acceleration was greater than both longitudinal and vertical acceleration in the majority of the cases analyzed, with the exception of the pitch-pulse and 2-*g* turn maneuvers, in which more significant vertical acceleration was present. Peaks in the acceleration PSD were seen at frequencies of approximately 65, 85, 105–110, 200, 500, and 1000 Hz. The largest random vibration levels below approximately 40 Hz occurred during takeoff and landing. From greater than 40 Hz to approximately 300 Hz, the Mach 0.9, transonic flight PSD levels were greatest. Random vibration levels were larger for transonic flight than for subsonic or supersonic flight. From approximately 300 to 1325 Hz, the takeoff produced the largest random vibration levels. Significant vibration levels were also encountered during sideslip maneuvers and landing, possibly because of vortex shedding from the nosewheel landing gear door impinging on the FTF–II.

# REFERENCES


1. Richwine, David M., *F-15B/Flight Test Fixture II: A Test Bed for Flight Research*, NASA TM-4782, 1996.

2. NASA Dryden Flight Research Center, *Environmental Testing Electronic and Electromechanical Equipment*, Process Specification No. 21-2, May 23, 1989.

3. Meyer, Robert R., Jr., *A Unique Flight Test Facility: Description and Results*, NASA TM-84900, 1982.

4. *MATLAB*®, Version 5.3, The MathWorks, Inc., Natick, Massachusetts, Nov. 2000.

5. Hoerner, Sighard F., *Fluid-Dynamic Drag: Practical Information on Aerodynamic Drag and Hydrodynamic Resistance*, Self-published work, Library of Congress Card Number 64-19666, Washington, D.C., 1965.


EC00 0282-01

Figure 1. The NASA F-15B/Flight Test Fixture II test bed in flight.

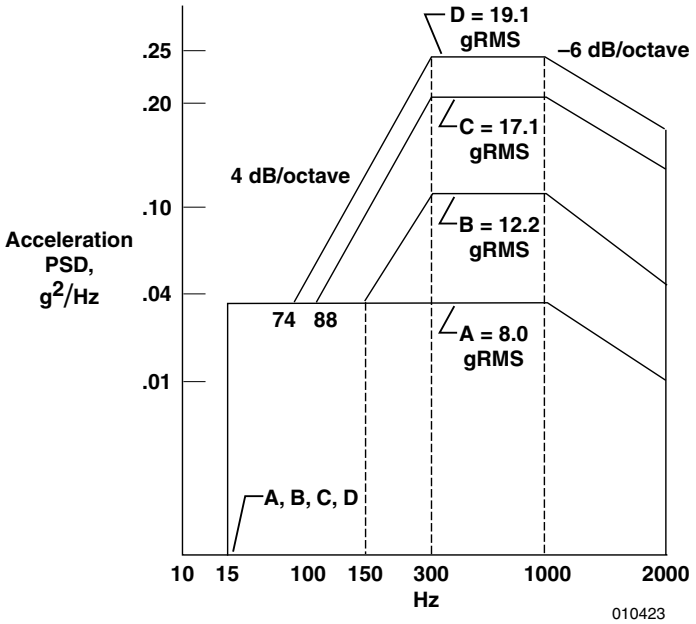


Figure 2. NASA Dryden random vibration shake test curves A–D.

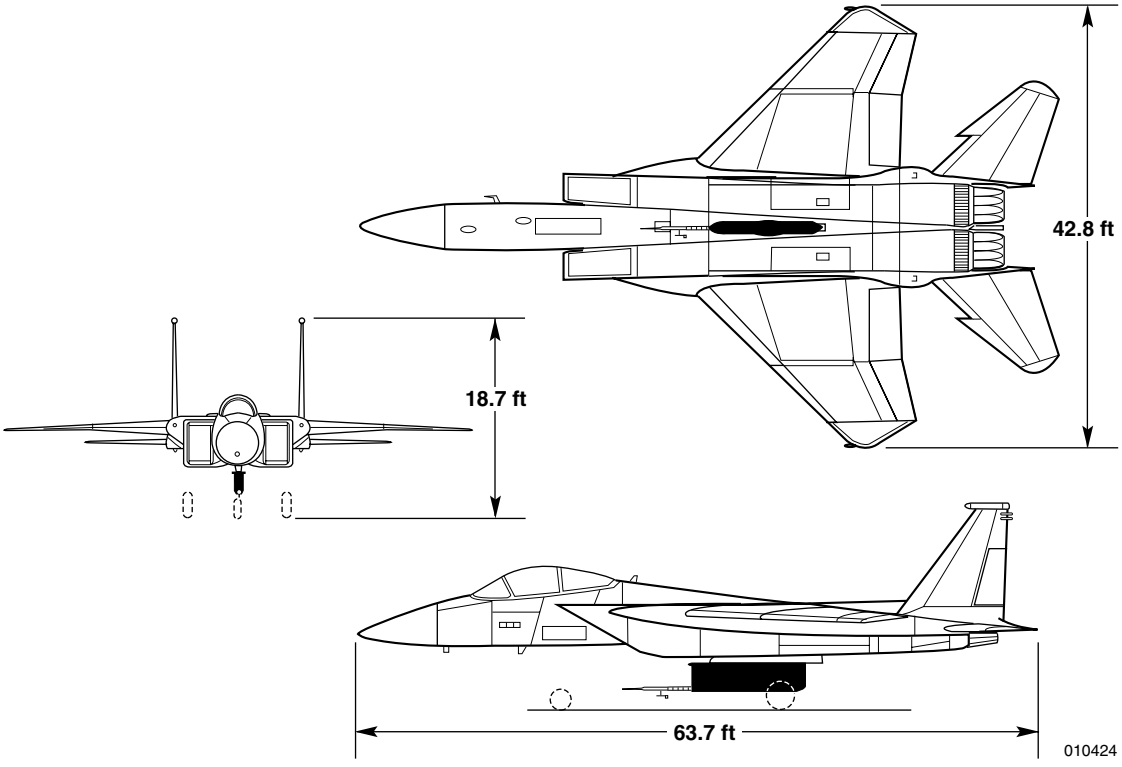


Figure 3. Three-view drawing of the NASA F-15B airplane with the FTF–II installed.

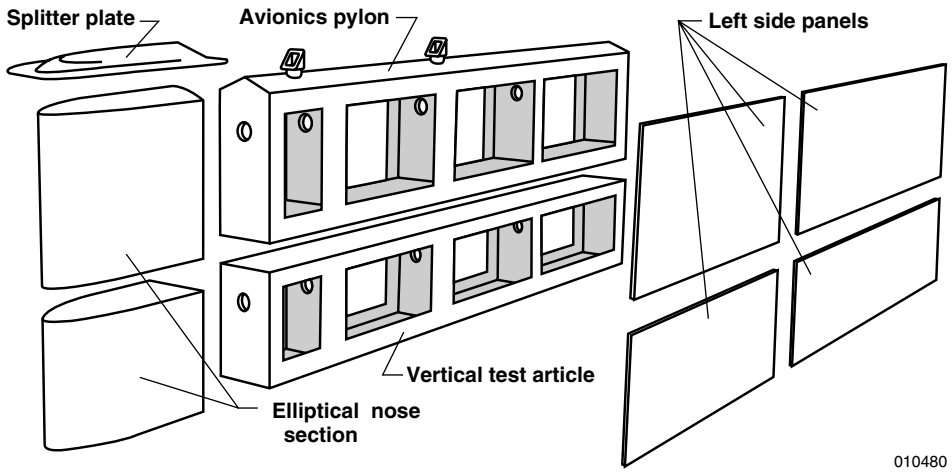


(a) Exploded isometric view.

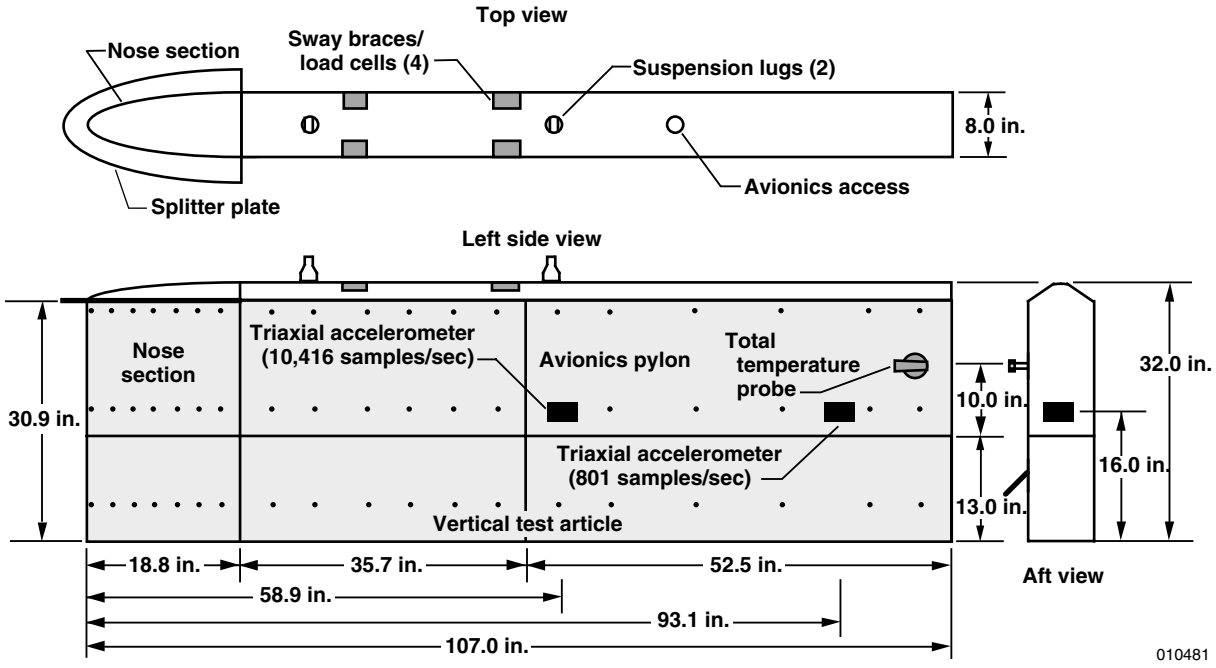


(b) Three-view.

Figure 4. Flight Test Fixture II.

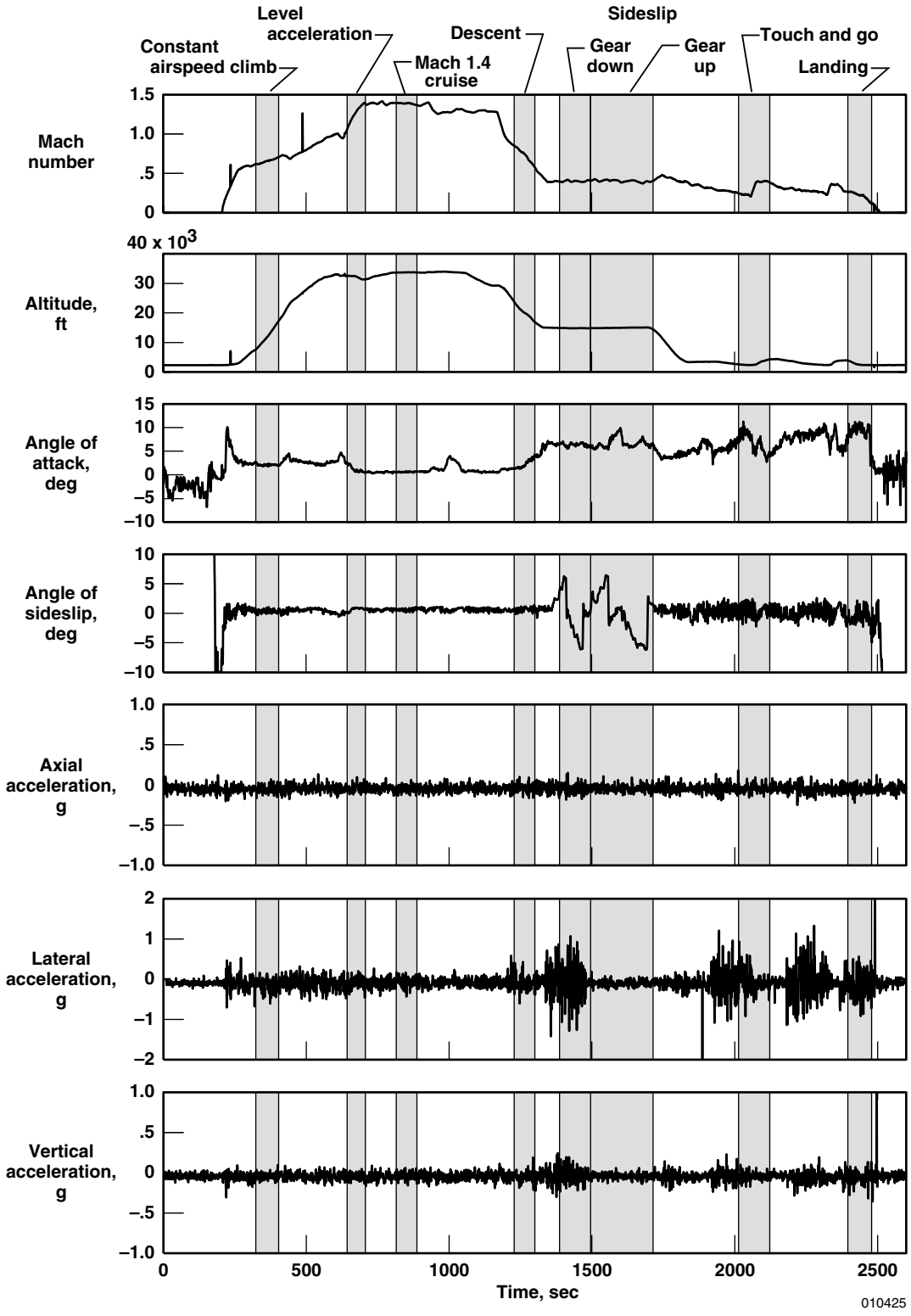


Figure 5. Longitudinal, lateral, and vertical acceleration as a function of time for a complete flight profile (flight 165).

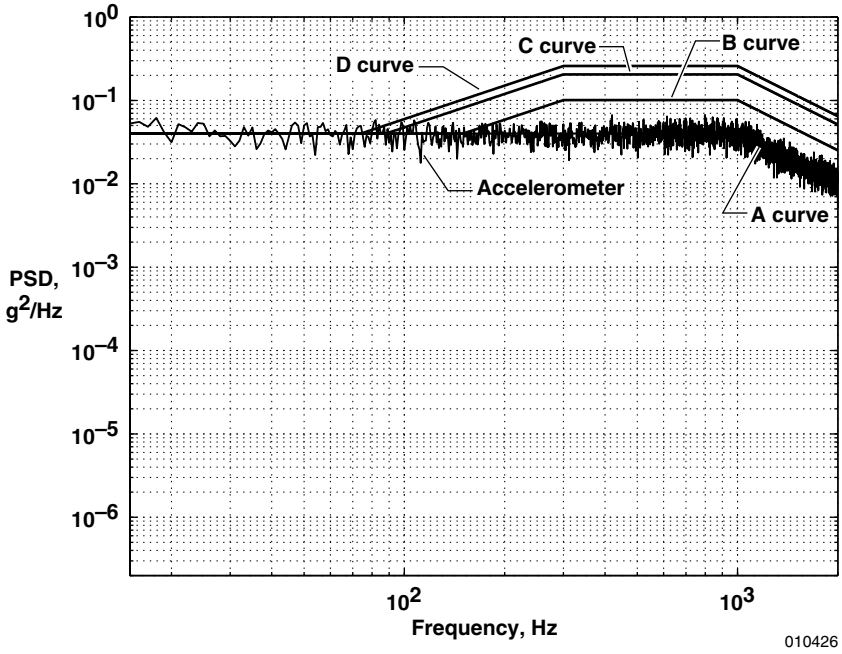


Figure 6. The PSD results of a "curve A" shake test on an accelerometer.

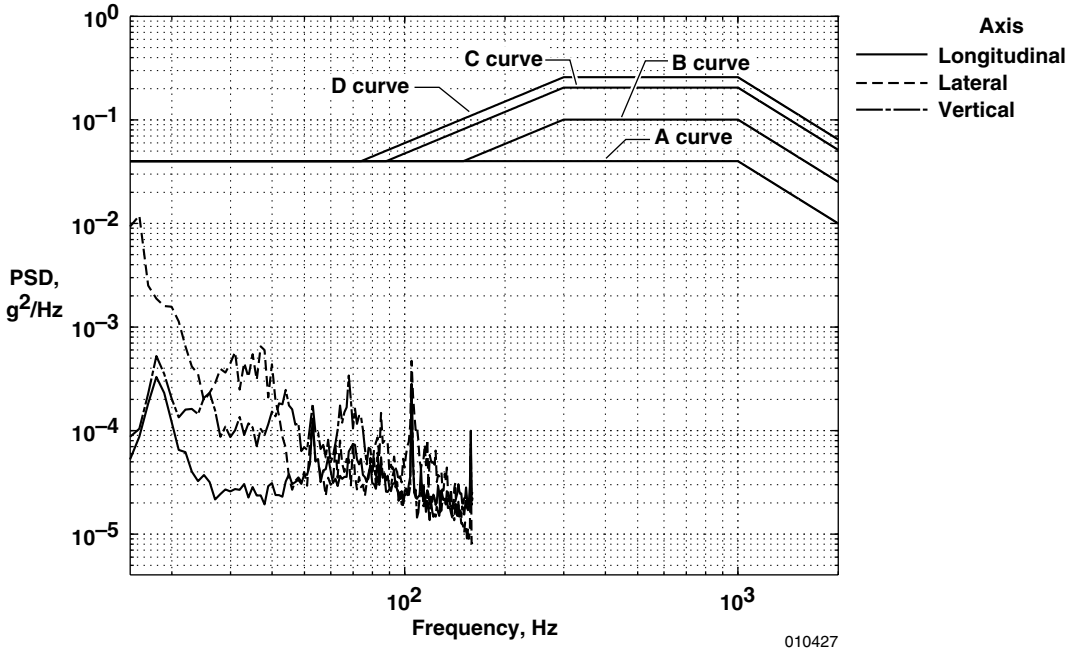


(a) Takeoff.

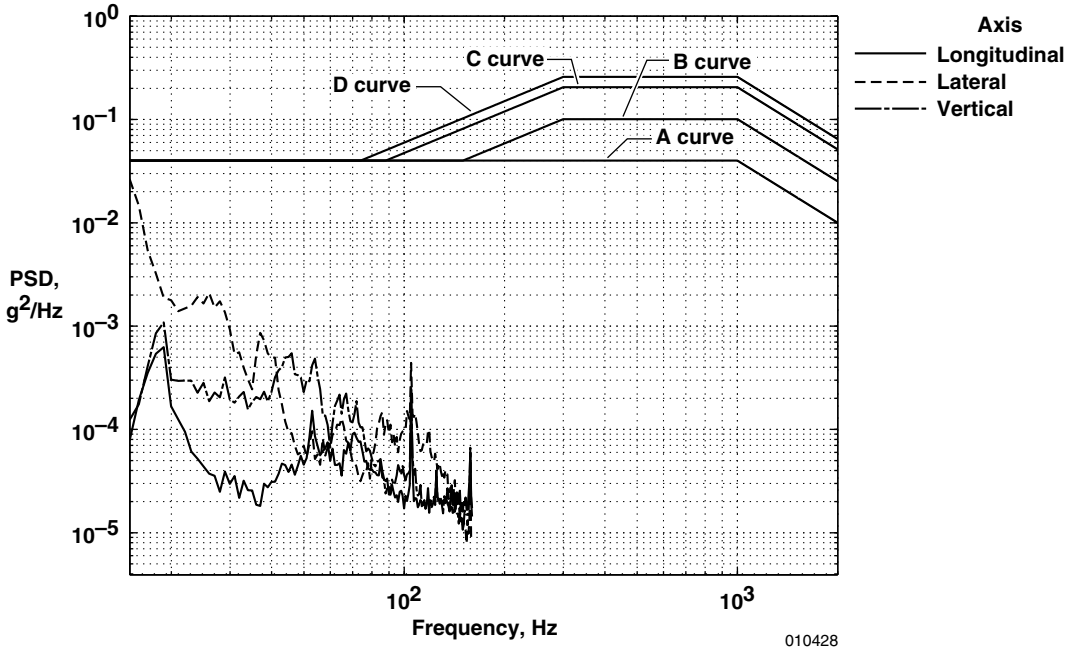


(b) Landing.

Figure 7. Comparison of longitudinal, lateral, and vertical acceleration PSD as a function of frequency (flight 165).

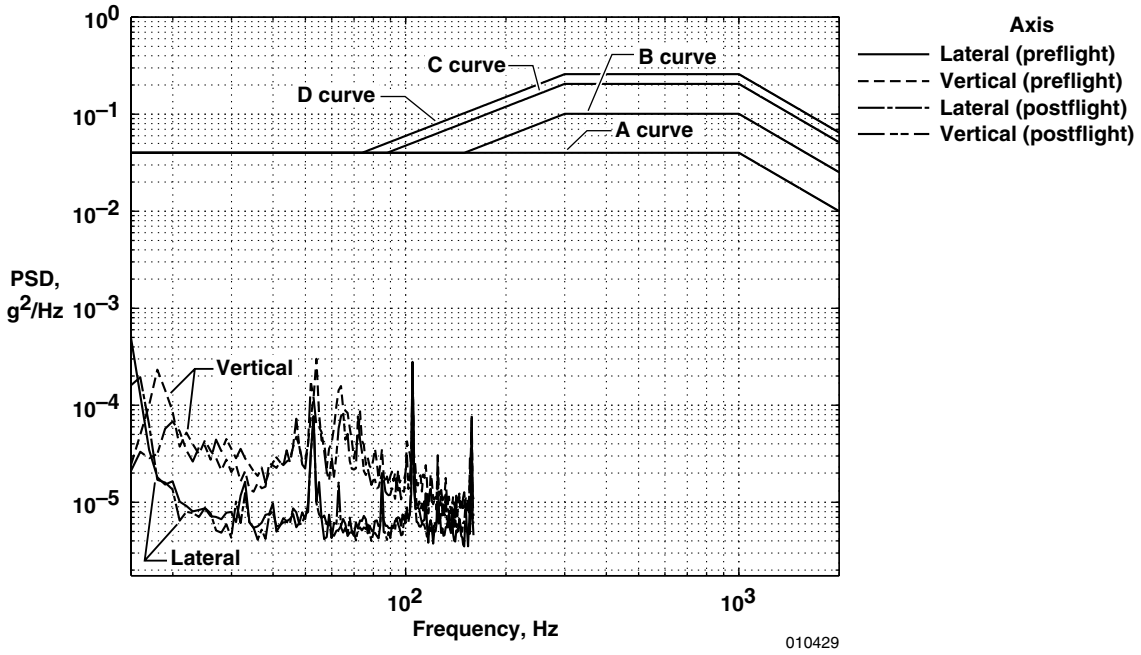


Figure 8. Lateral and vertical acceleration PSD for taxi.

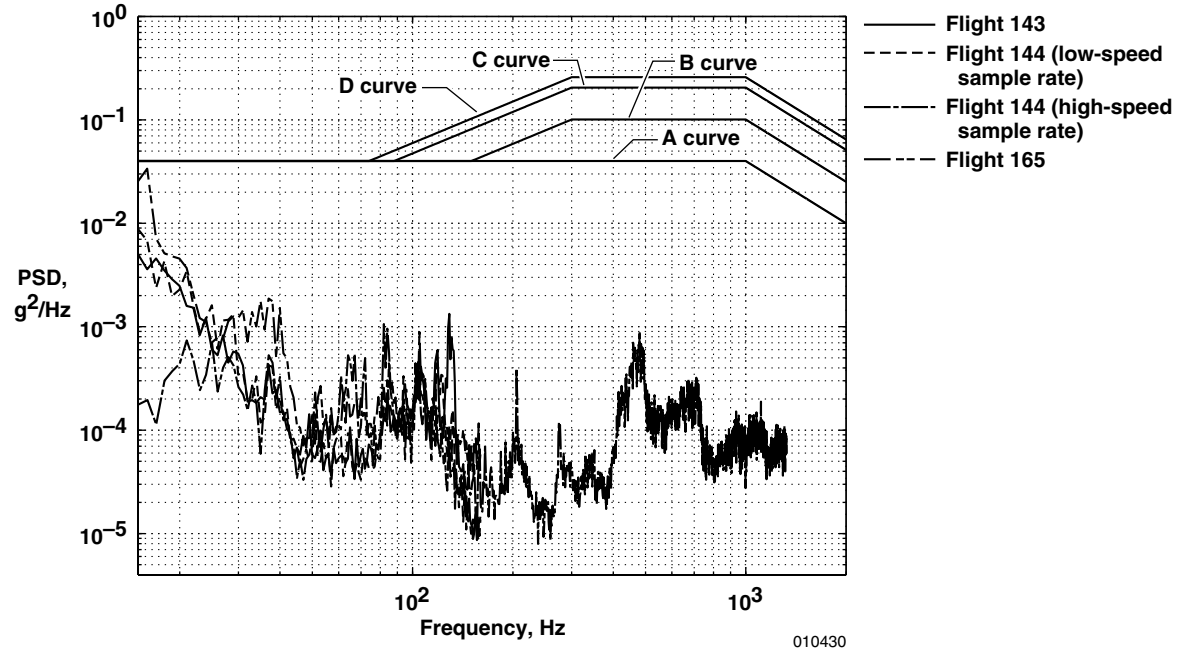


Figure 9. Lateral acceleration PSD for takeoff.

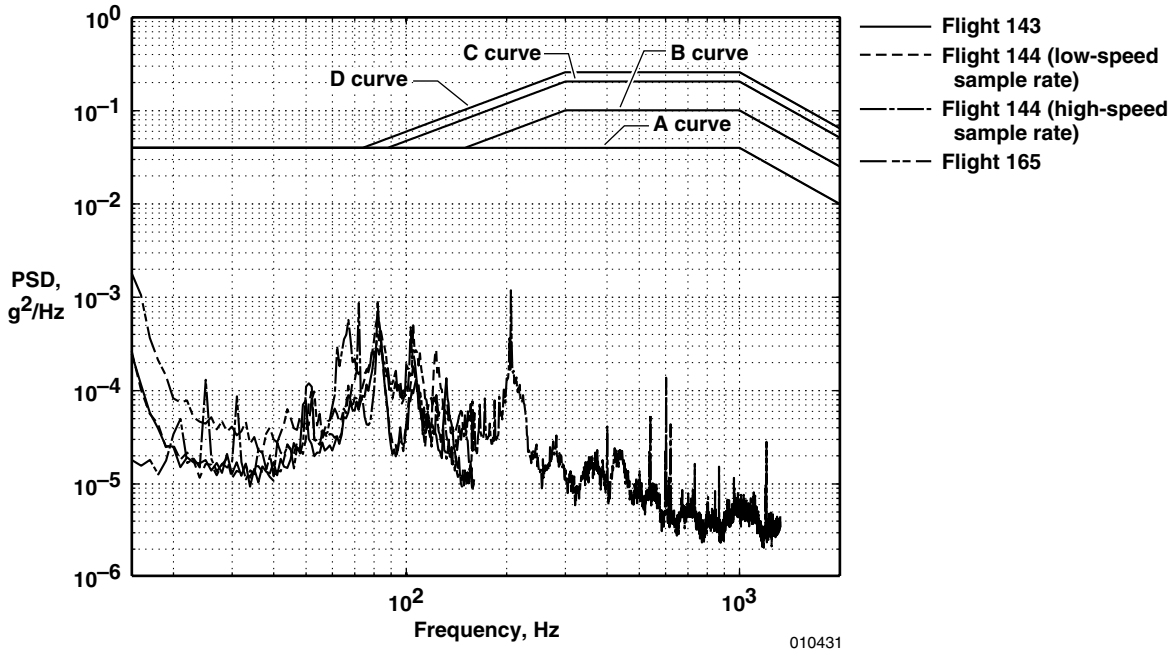


Figure 10. Lateral acceleration PSD for steady climbing flight.

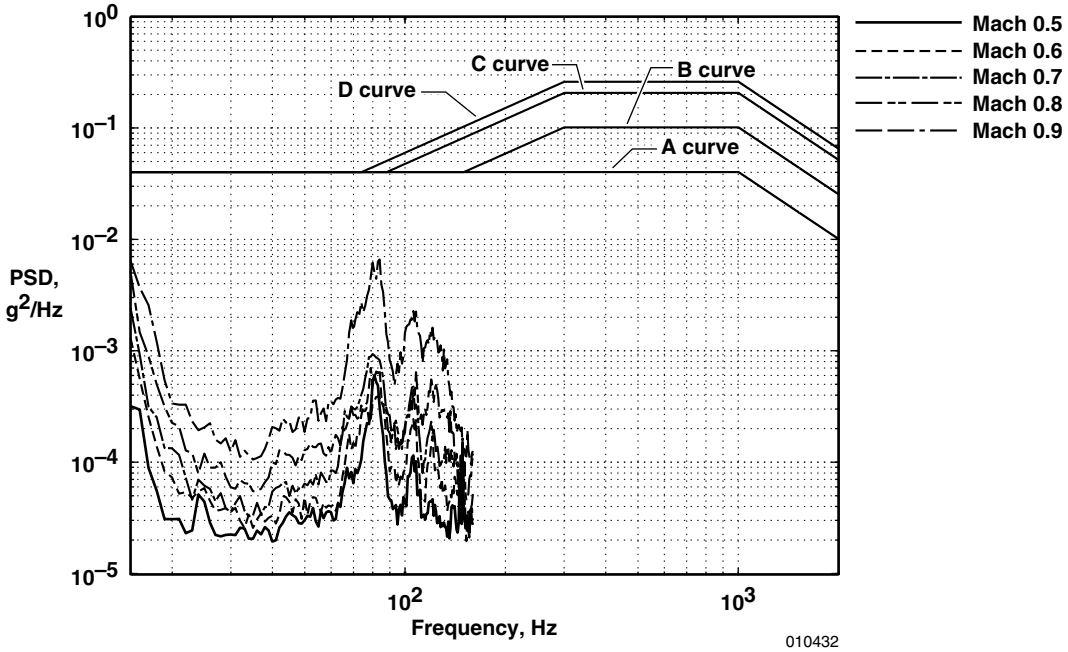


Figure 11. Lateral acceleration PSD for level subsonic flight.

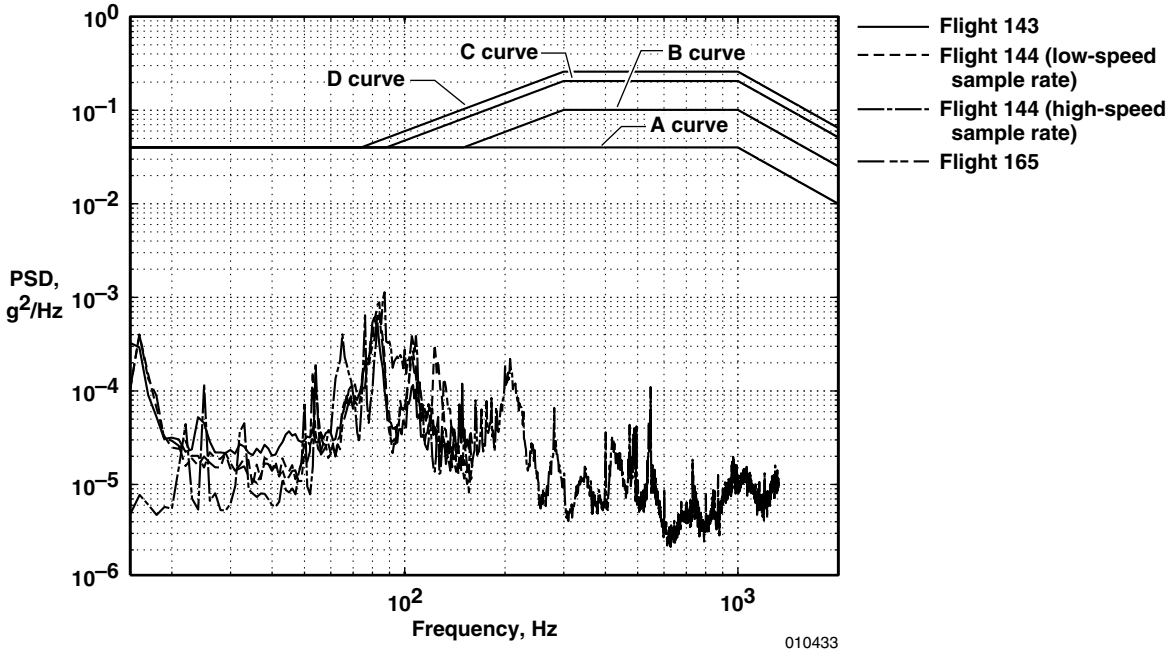


Figure 12. Lateral acceleration PSD for level flight at Mach 0.5.

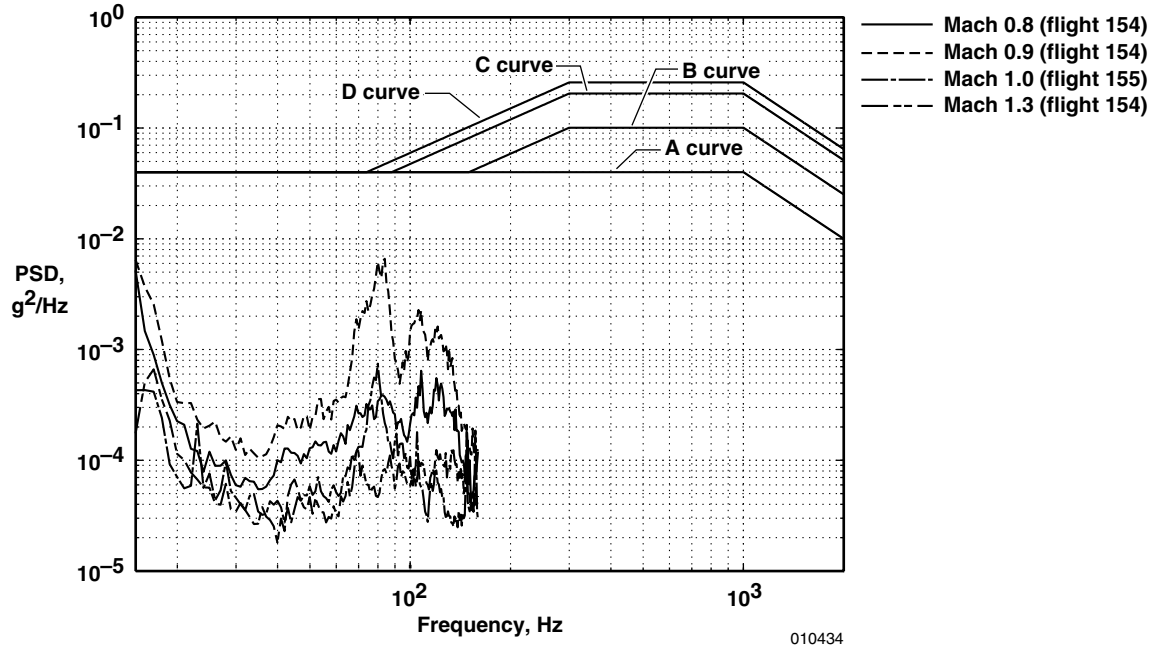


Figure 13. Lateral acceleration PSD for level transonic flight.

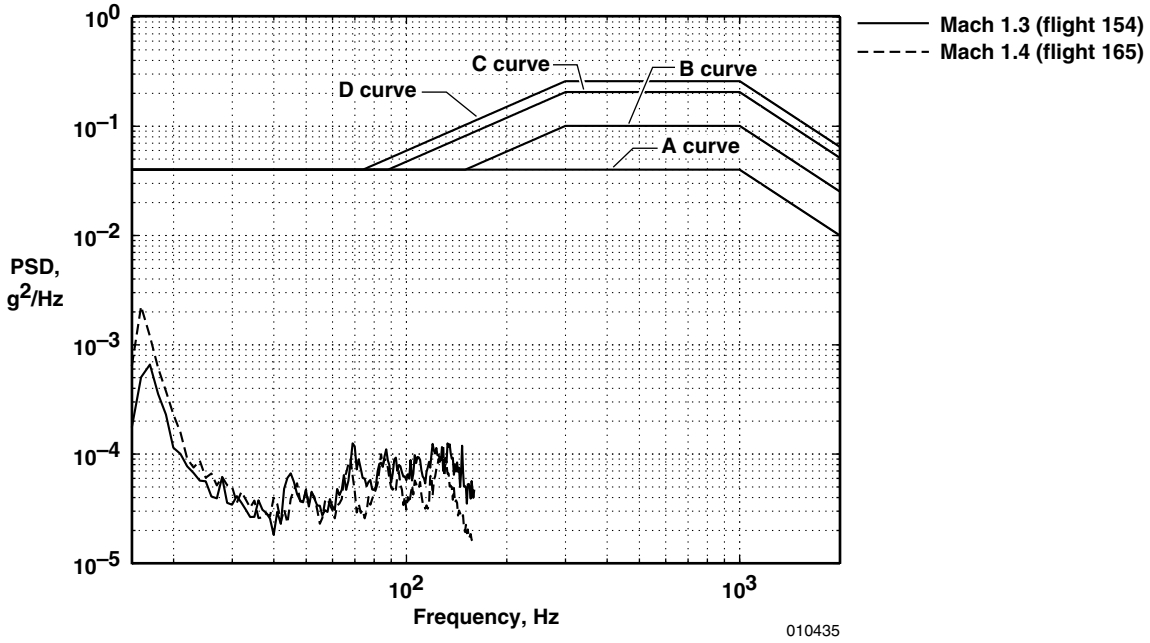


Figure 14. Lateral acceleration PSD for level supersonic flight.

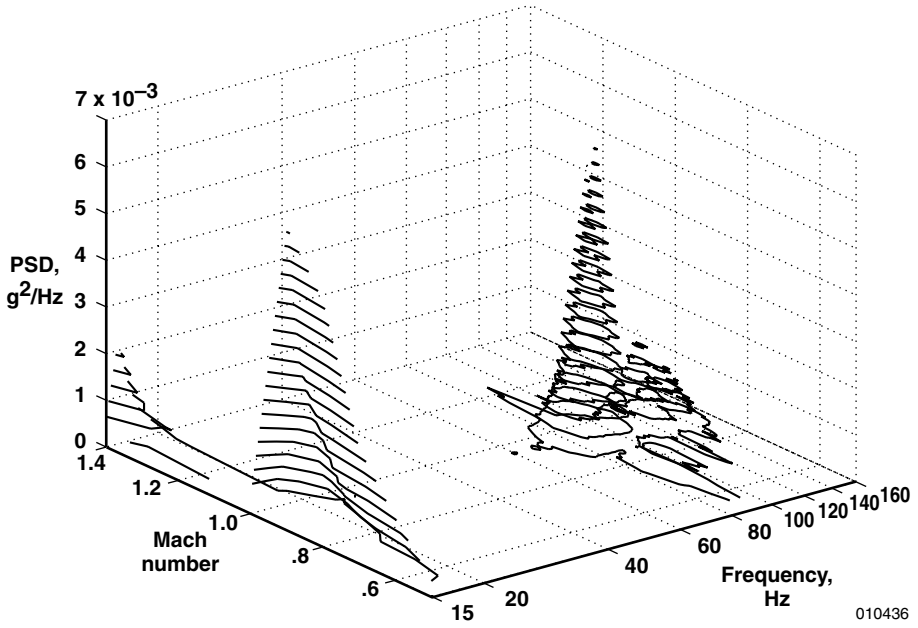


(a) Three-dimensional contour plot.

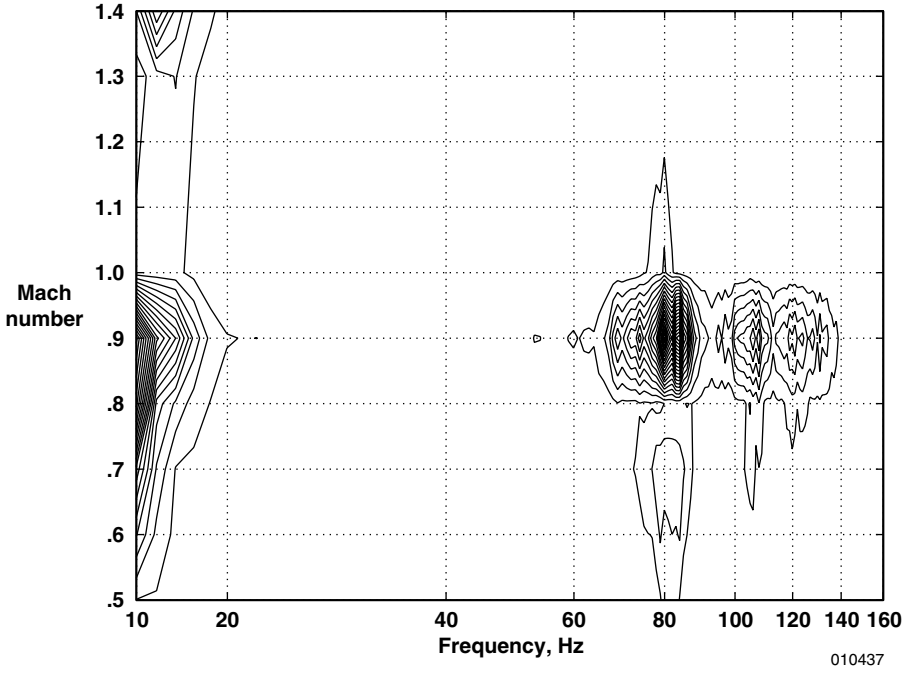


(b) Two-dimensional contour plot.

Figure 15. Lateral acceleration PSDs for various Mach numbers.

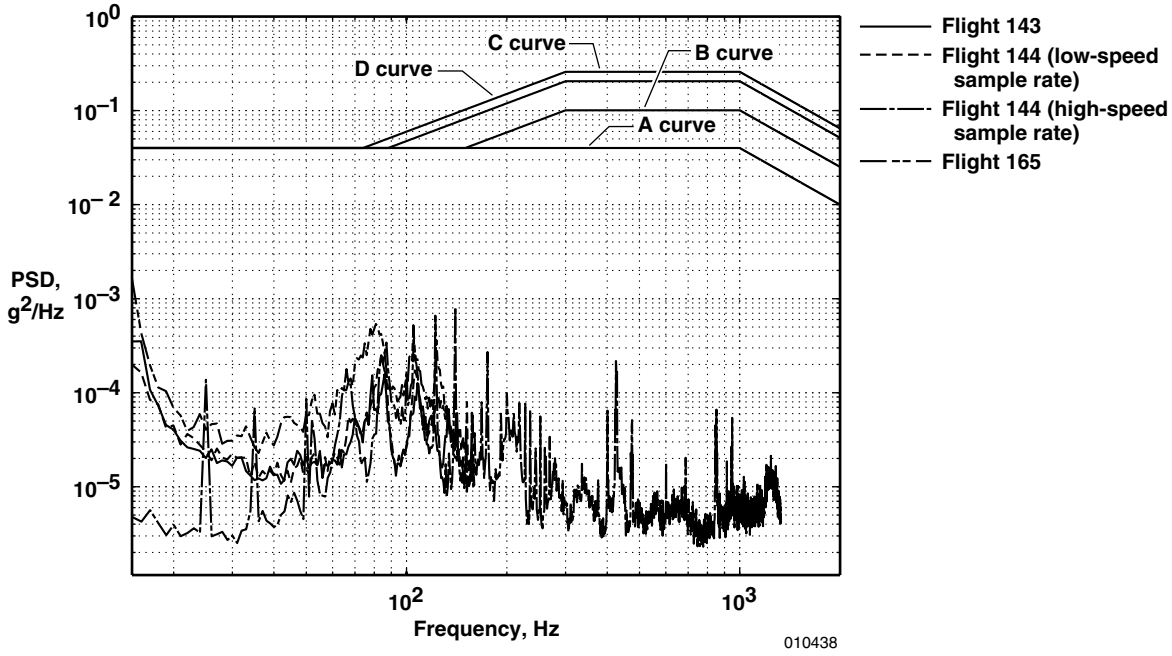


Figure 16. Lateral acceleration PSD for descent.

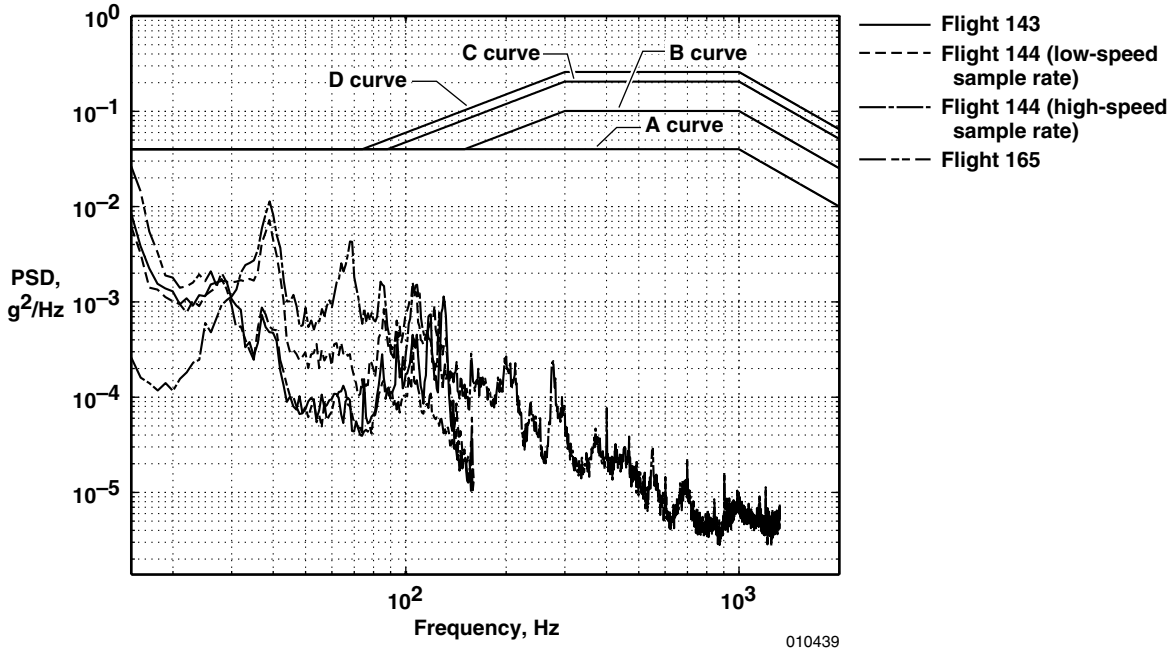


(a) Lateral acceleration.

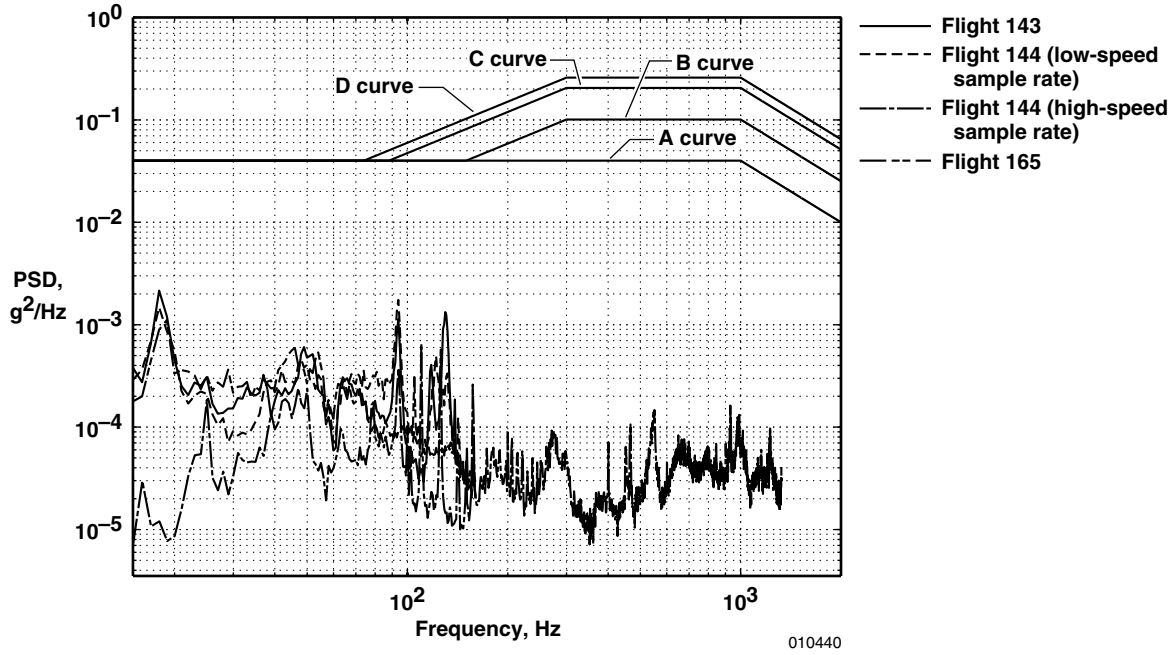


(b) Vertical acceleration.

Figure 17. Acceleration PSDs for landing.

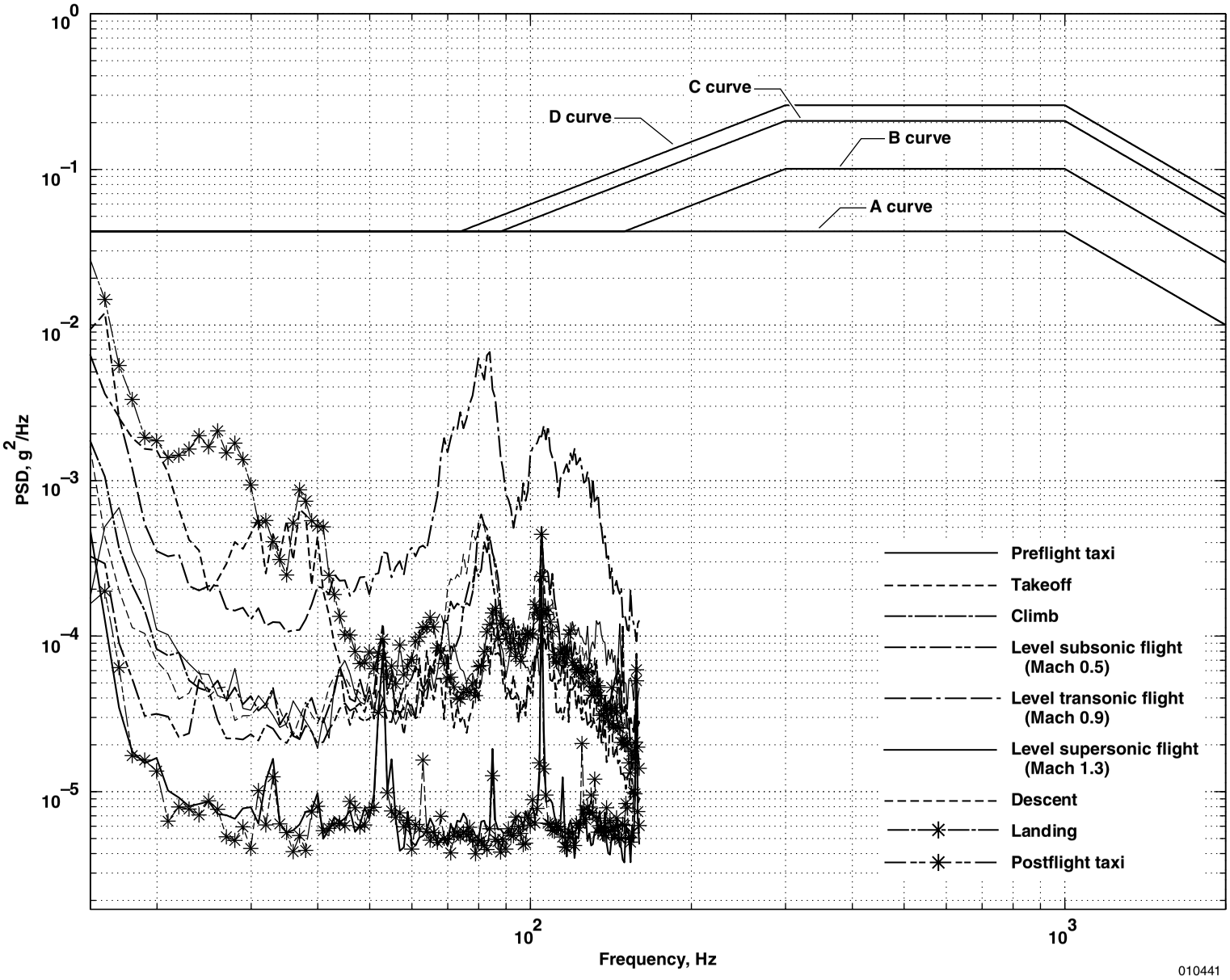


(a) Low-speed data.

Figure 18. Comparison of lateral acceleration PSD for steady-state flight conditions.

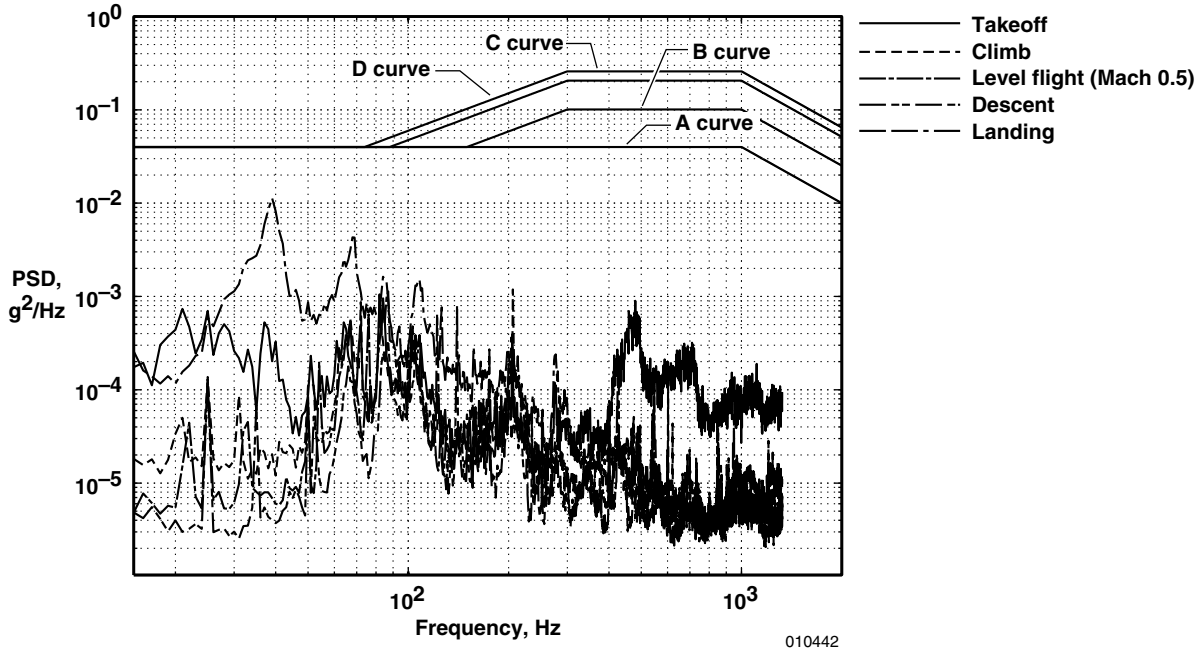


(b) High-speed data.

Figure 18. Concluded.

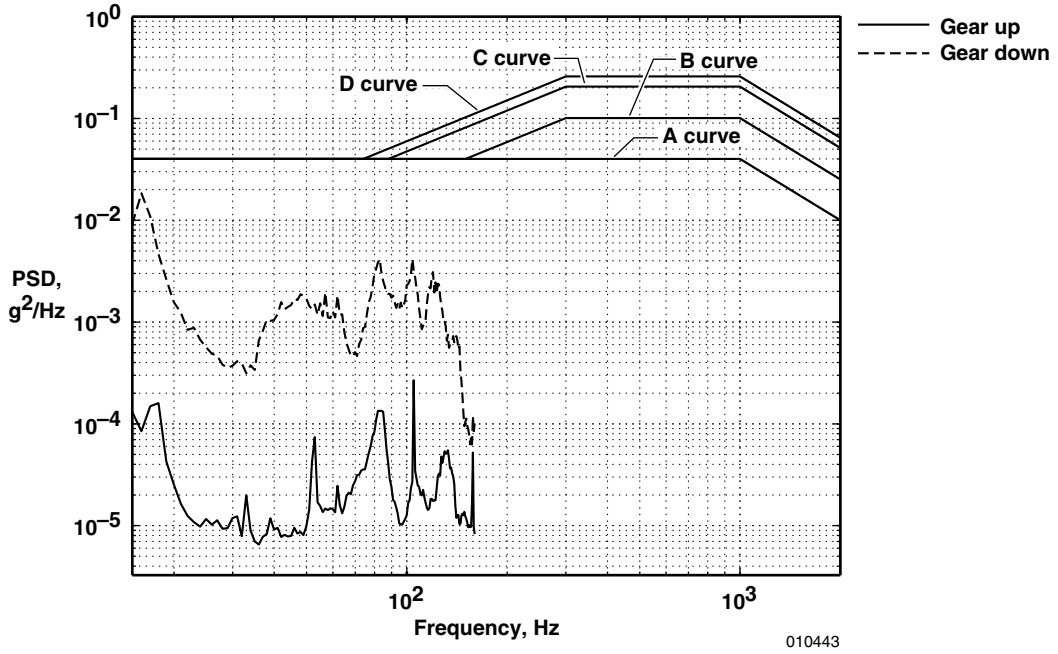


Figure 19. Lateral acceleration PSD for a steady-heading sideslip.

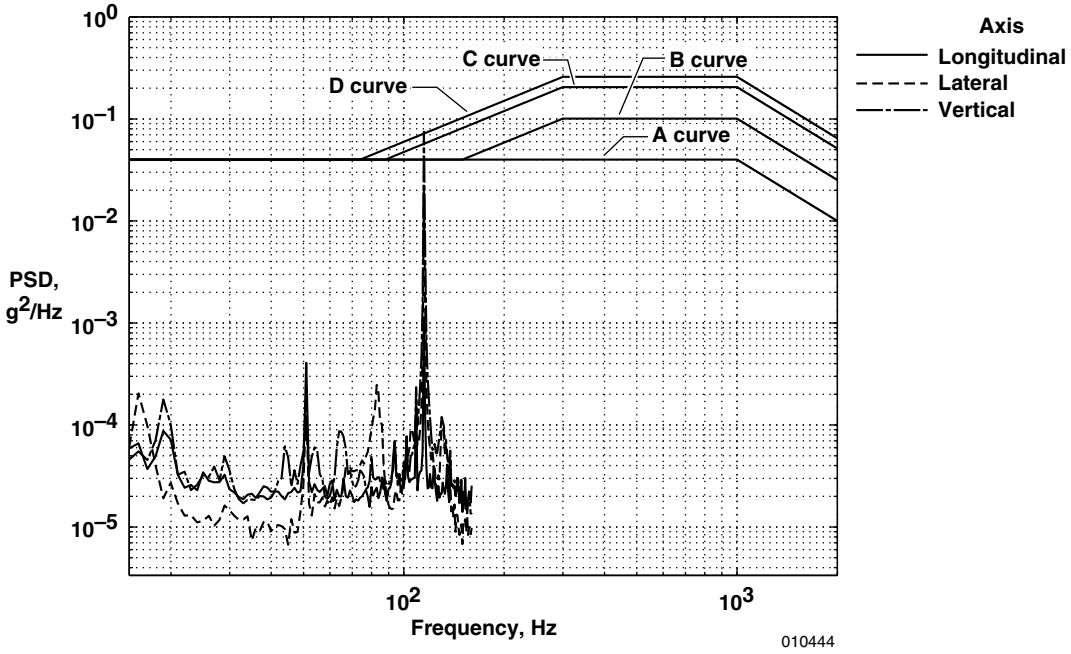


Figure 20. Acceleration PSD for a pitch pulse maneuver (flight 143).

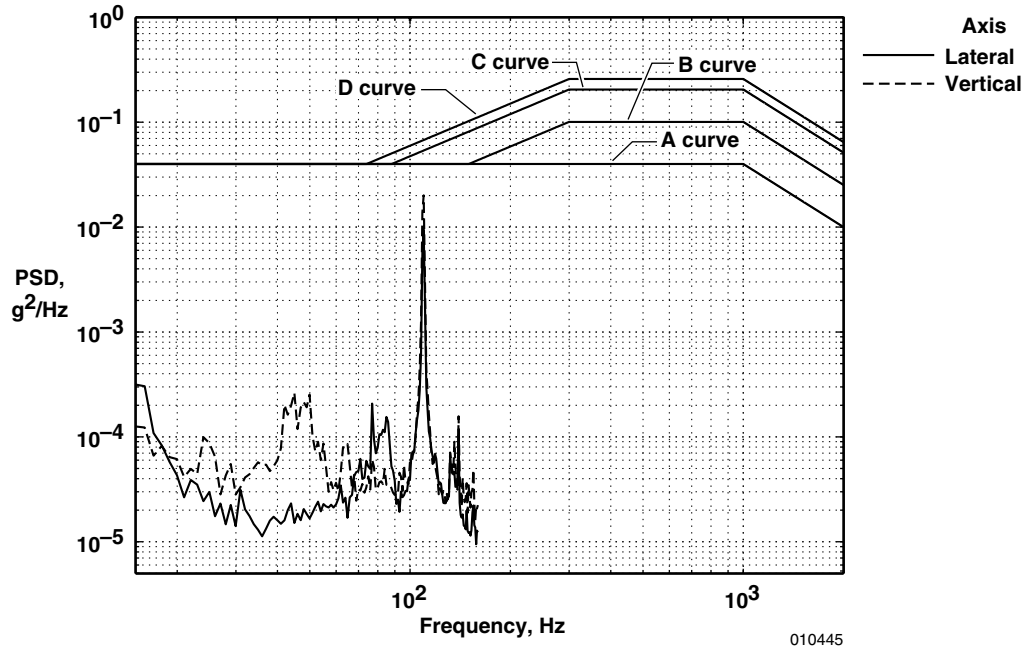


Figure 21. Lateral and vertical acceleration PSD for a level 2-*g* turn (flight 143).

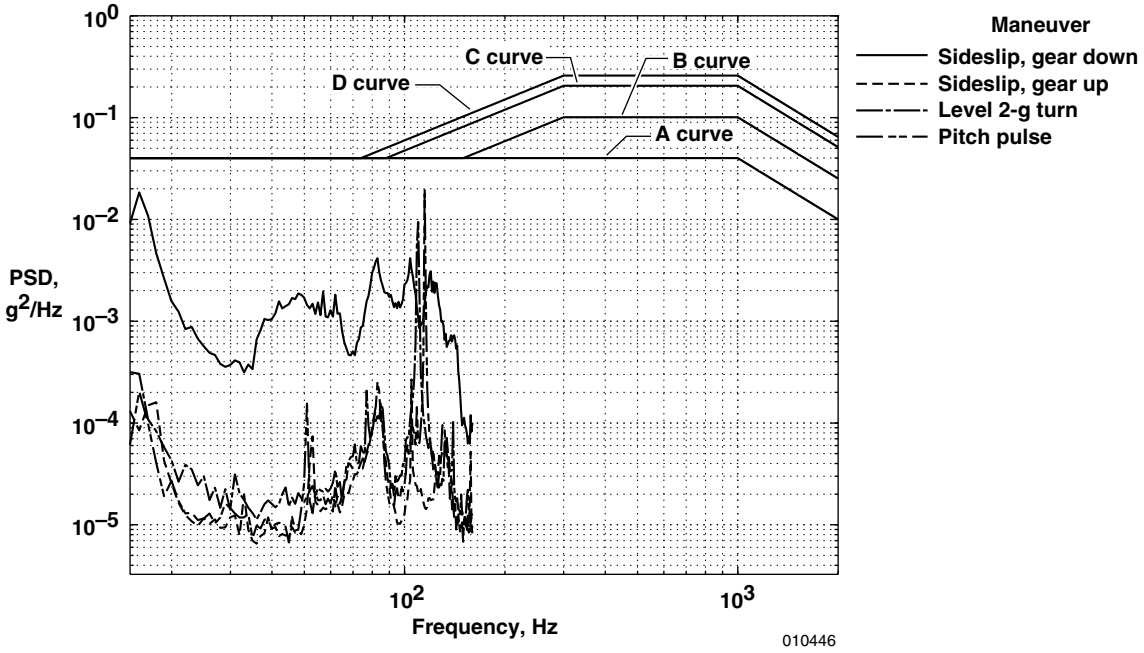


Figure 22. Comparison of lateral acceleration PSD for various flight maneuvers.

# REPORT DOCUMENTATION PAGE

Form Approved
OMB No. 0704-0188



| 1. AGENCY USE ONLY (Leave blank) | 2. REPORT DATE | 3. REPORT TYPE AND DATES COVERED |
|---|---|---|
| | February 2002 | Technical Memorandum |

**4. TITLE AND SUBTITLE**

In-Flight Vibration Environment of the NASA F-15B Flight Test Fixture

**5. FUNDING NUMBERS**

WU 710-35-14-M1-00-38-00-S-000

**6. AUTHOR(S)**

Stephen Corda, Russell J. Franz, James N. Blanton, M. Jake Vachon, and James B. DeBoer

**7. PERFORMING ORGANIZATION NAME(S) AND ADDRESS(ES)**

NASA Dryden Flight Research Center
P.O. Box 273
Edwards, California 93523-0273

**8. PERFORMING ORGANIZATION REPORT NUMBER**

H-2468

**9. SPONSORING/MONITORING AGENCY NAME(S) AND ADDRESS(ES)**

National Aeronautics and Space Administration
Washington, DC 20546-0001

**10. SPONSORING/MONITORING AGENCY REPORT NUMBER**

NASA/TM-2002-210719

**11. SUPPLEMENTARY NOTES**

**12a. DISTRIBUTION/AVAILABILITY STATEMENT**

Unclassified—Unlimited
Subject Category: 05

This report is available at http://www.dfrc.nasa.gov/DTRS/

**12b. DISTRIBUTION CODE**

**13. ABSTRACT (Maximum 200 words)**

Flight vibration data are analyzed for the NASA F-15B/Flight Test Fixture II test bed. Understanding the in-flight vibration environment benefits design and integration of experiments on the test bed. The power spectral density (PSD) of accelerometer flight data is analyzed to quantify the in-flight vibration environment from a frequency of 15 Hz to 1325 Hz. These accelerometer data are analyzed for typical flight conditions and maneuvers. The vibration data are compared to flight-qualification random vibration test standards. The PSD levels in the lateral axis generally are greater than in the longitudinal and vertical axes and decrease with increasing frequency. At frequencies less than approximately 40 Hz, the highest PSD levels occur during takeoff and landing. Peaks in the PSD data for the test fixture occur at approximately 65, 85, 105–110, 200, 500, and 1000 Hz. The pitch-pulse and 2-*g* turn maneuvers produce PSD peaks at 115 Hz. For cruise conditions, the PSD level of the 85-Hz peak is greatest for transonic flight at Mach 0.9. From 400 Hz to 1325 Hz, the takeoff phase has the highest random vibration levels. The flight-measured vibration levels generally are substantially lower than the random vibration test curve.

**14. SUBJECT TERMS**

F-15B flight test fixture, Flight test, Power spectral density, Random vibration, Vibration flight data

**15. NUMBER OF PAGES**

28

**16. PRICE CODE**

A03

| 17. SECURITY CLASSIFICATION OF REPORT | 18. SECURITY CLASSIFICATION OF THIS PAGE | 19. SECURITY CLASSIFICATION OF ABSTRACT | 20. LIMITATION OF ABSTRACT |
|---|---|---|---|
| Unclassified | Unclassified | Unclassified | Unlimited |